Supporting Information: A One-Pot-One-Reactant Synthesis of Platinum Compounds at the Nanoscale- Supplementary Information

Contents

1. Fluorescence-Detected X-Ray Absorption Spectroscopy (FD-XAS) Data

a. Further Pt L_{III} edge data and Raman Spectroscopy

Table S-1: Shifts of excitaiton energy estimated from the Pt L_{III} edge for the materials in SWNTs compared to known standards. Where applicable the shift in the G-band of materials compared to that of a pristine SWNT as shown by Raman spectroscopy have been recorded, and direction of charge transfer

Sample	Original excitation edge / eV (shift with respect to metallic Pt / eV)	G-band position / cm^{-1} (shift with respect to empty nanotube / cm^{-1})	Direction of electron transfer (if applicable)
Pt wire	11561.30 ± 0.70 (0)	N/A	
$Pt(acac)_2I_2$@SWNT	11561.84 ± 0.03 (0.54)	1594.5 (+5.6)	Pt ← SWNT
$Pt(acac)_2$	11562.16 ± 0.74 (0.86)	N/A	
PtI_2	11562.22 ± 0.39 (0.92)	N/A	
Pt@SWNT	11562.30 ± 0.21 (1.00)	1584.5 (-4.4)	Pt → SWNT

PtI_2@SWNT	11562.52 ± 0.24 (1.22)	1588.9 (0)	No transfer observed
$Pt(acac)_2$@SWNT	11562.67 ± 0.20 (+1.37)	1590.0 (+1.1)	
$Pt(acac)_2(SCN)_2$@SWNT	11563.00 ± 0.13 (1.70)	1583.9 (-5.0)	
PtI_4	11563.19 ± 0.26 (1.89)	N/A	
$Pt(acac)_2I_2$	11563.34 ± 0.24 (2.04)	N/A	
PtS_x@SWNT	11563.58 ± 0.22 (2.28)	1588.9 (0)	
$Pt(acac)_2(SCN)_2$	11563.63 ± 0.12 (2.33)	N/A	
SWNT	N/A	1588.9	

FD-XAS measurements of Pt containing compounds in SWNTs against controls at the Pt L_{III} edge were acquired on beamline B28 at the ESRF. Samples were prepared by mounting a solid sample on silicon (100) supports. Raman spectroscopy was recorded using a HoribaJY LabRAM HR spectro-meter, laser wavelength 532 nm. Samples were recorded by dispersing in propan-2-ol and drop-casting onto silicon (100) supports. All FD-XAS and Raman spectra were recorded room temperature.

b. Extended Pt L_{III} edge data

i. Stepwise formation of Pt containing compounds in SWNTs.

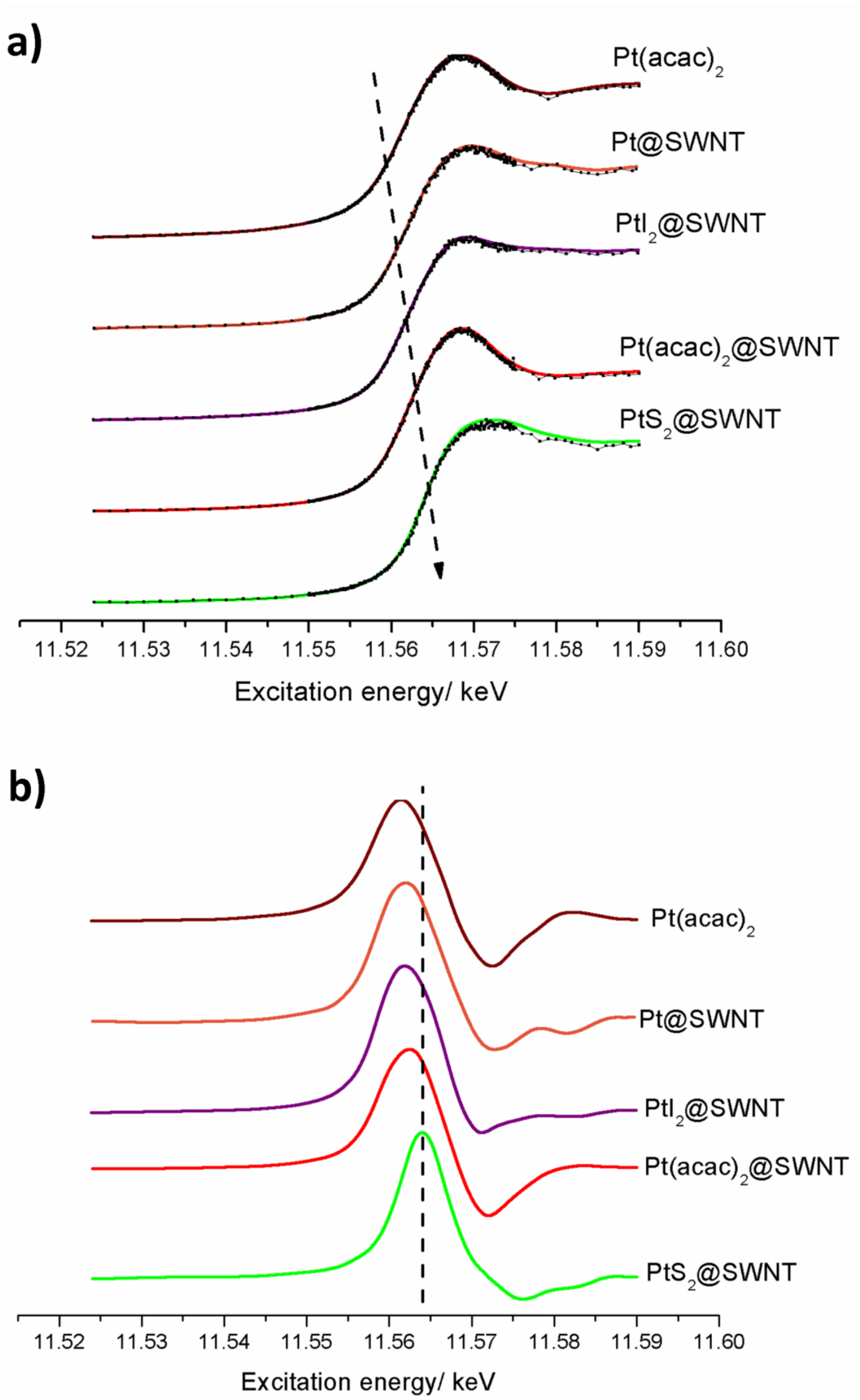

Figure S-1: Pt L_{III} edge spectra of Pt materials formed using a stepwise approach (a). The raw data is shown by the black plot, and the smoothed data is overlaid in colour in each case.

The first derivative (b) of each smoothed spectrum is shown, to determine the excitation edge position.

ii. One-pot formation of Pt and I containing compounds.

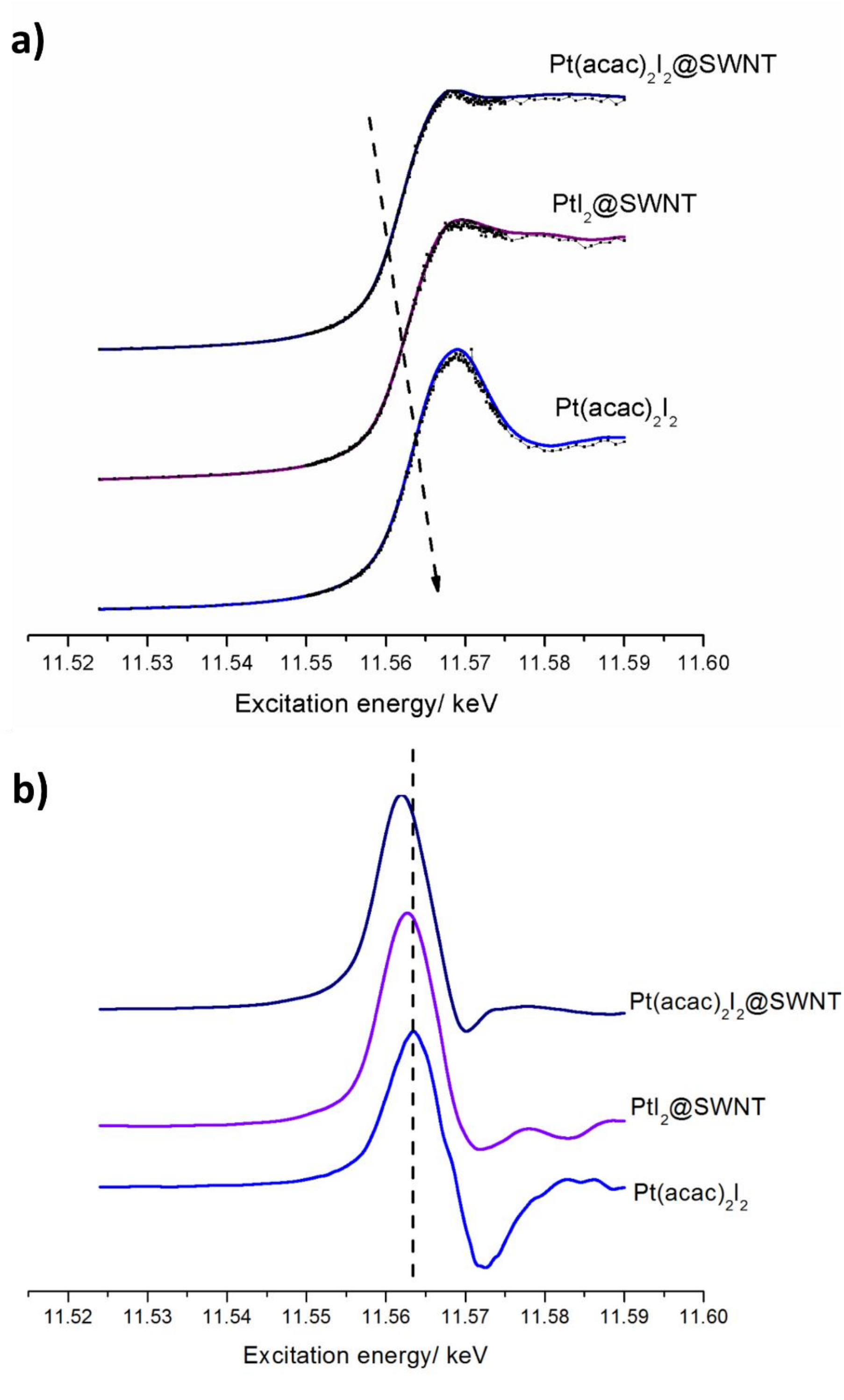

Figure S-2: Pt L_{III} edge spectra of Pt and I containing materials formed using a one-pot filling approach (a). The raw data is shown by the black plot, and the smoothed data is overlaid in colour in each case. The first derivative (b) of each smoothed spectrum is shown, to determine the excitation edge position.

iii. One pot formation of Pt and S containing compounds:

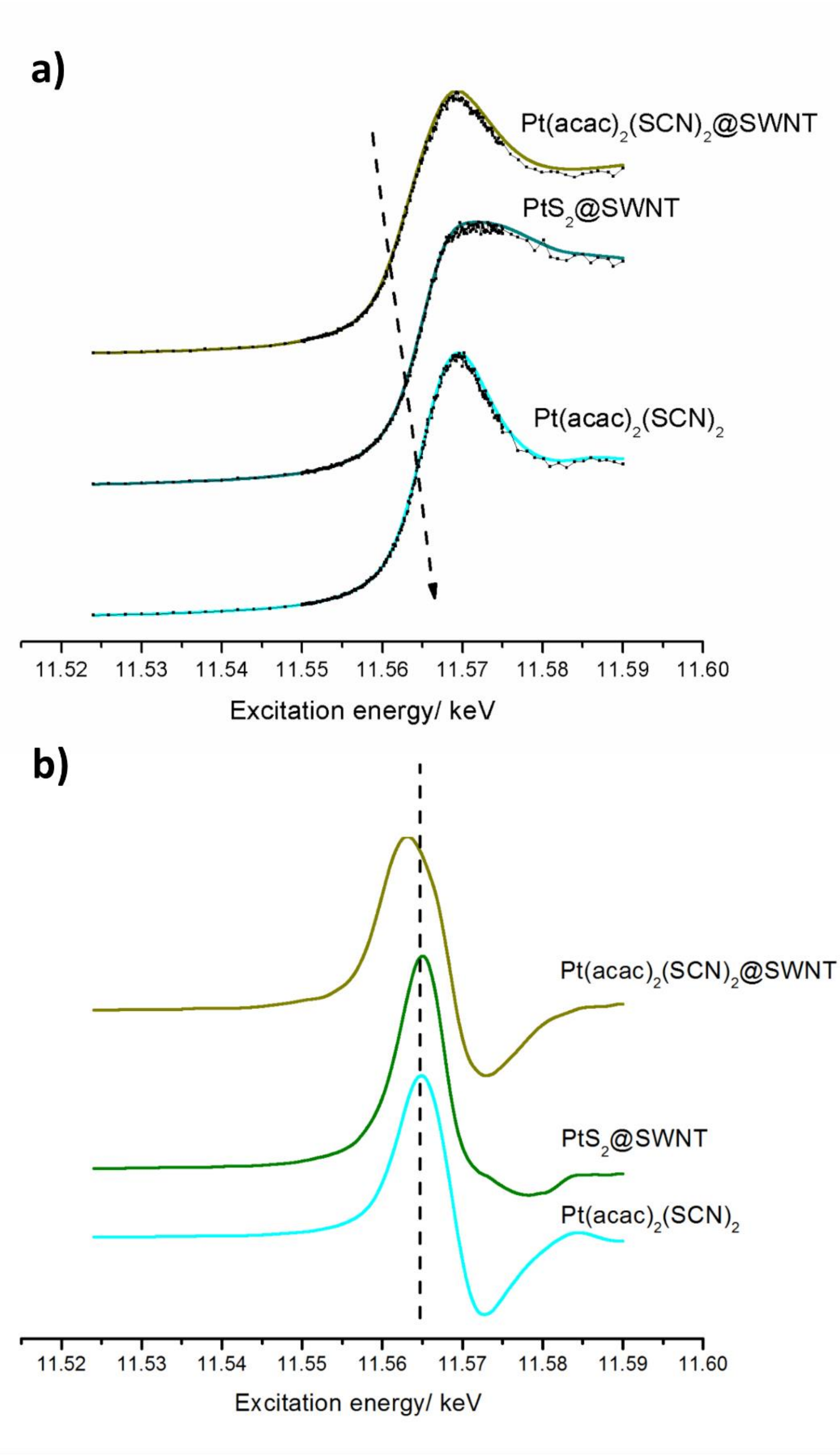

Figure S-3: Pt L_{III} edge spectra of Pt and S containing materials formed using a one-pot filling approach (a). The raw data is shown by the black plot, and the smoothed data is overlaid in

colour in each case. The first derivative (b) of each smoothed spectrum is shown, to determine the excitation edge position.

c. **Iodine L_{III} edge data**

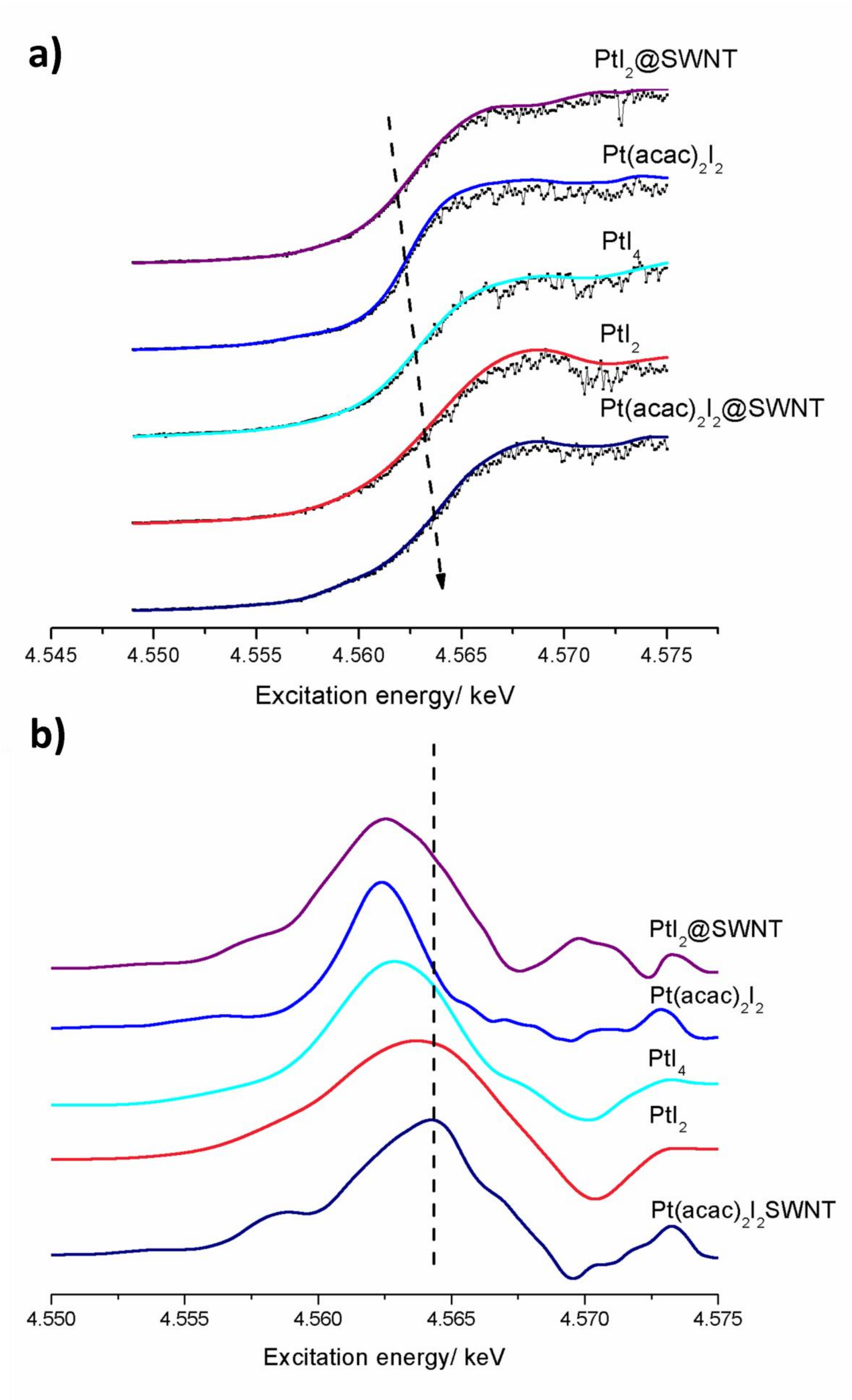

Figure S-4: FD-XAS showing the I L_3 edge of materials in SWNTs compared to that of bulk compounds (a), the raw data is shown by the black plot, and the smoothed data is overlaid in colour in each case. The first derivative (b) of each spectrum is shown, to determine the excitation edge position.

Table S-2: Shifts of excitaiton energy estimated from the I L_{III} edge energy for the materials in SWNTs compared bulk compounds.

Sample	Original excitation edge energy / eV
PtI_x@SWNT	4562.517 ± 0.03
$Pt(acac)_2I_2$	4562.593 ± 0.18
PtI_4	4563.094 ± 0.23
PtI_2	4563.861 ± 0.22
$Pt(acac)_2I_2$@SWNT	4564.199 ± 0.19

FD-XAS measurements of I containing compounds in SWNTs against controls at the I L_{III} edge were acquired on beamline B28 at the ESRF. All measurements were obtained and room temperature and samples were prepared by mounting solid material on silicon (100) supports.

d. **Sulfur K edge data**

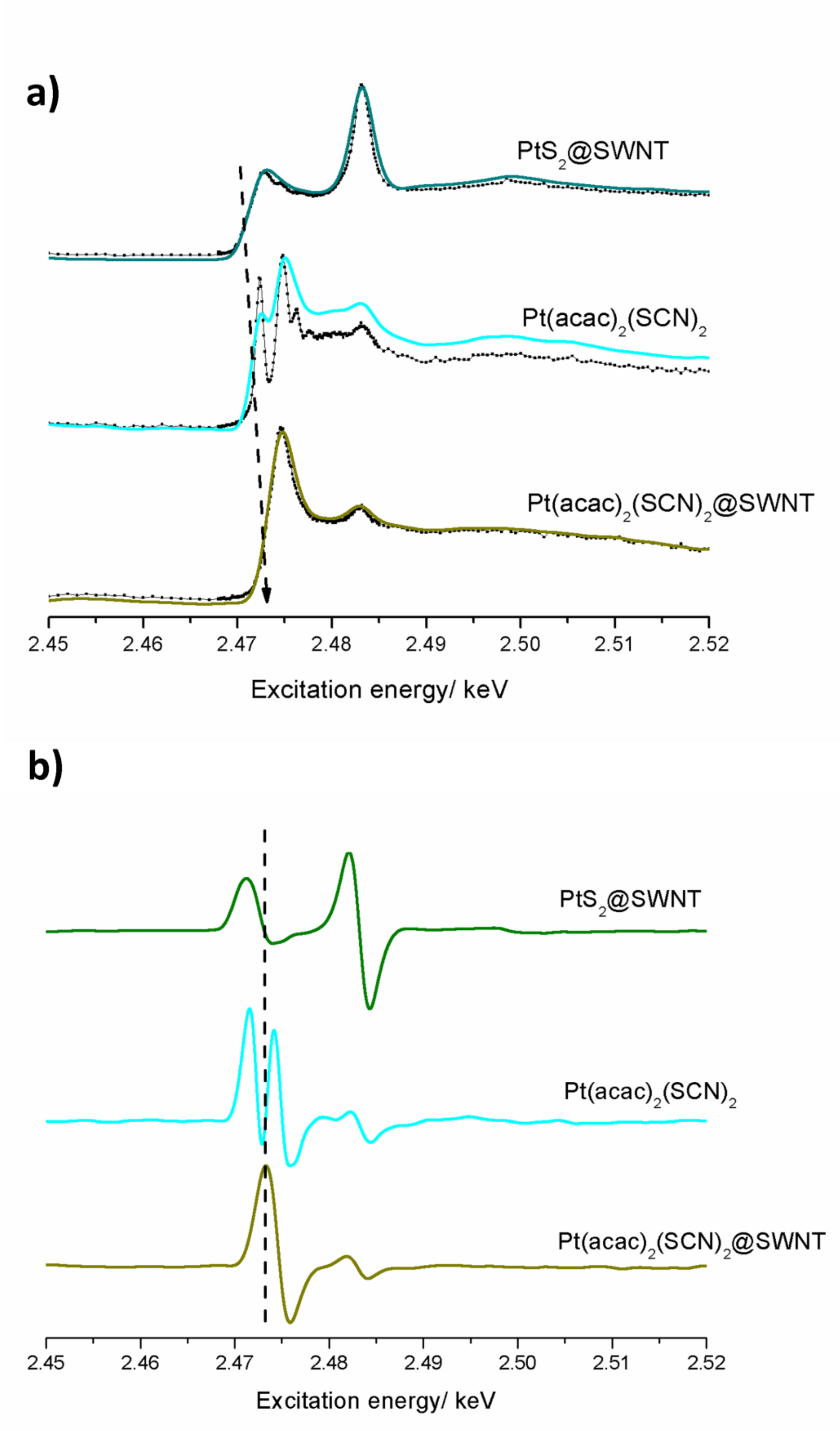

e.

Figure S-5: FD-XAS showing the S K edge of materials in SWNTs compared to that of bulk compounds, the raw data is shown by the black plot, and the smoothed data is overlaid in colour in each case. The first derivative (b) of each spectrum is shown, to determine the excitation edge position.

Table S-3: Shifts of excitaiton energy estimated from the S K edge energy for the materials in SWNTs compared to known standards.

Sample	Original excitation edge energy / eV
PtS_2@SWNT	2.470975 ± 0.24
$Pt(acac)_2(SCN)_2$	2.471571 ± 0.25
$Pt(acac)_2(SCN)_2$@SWNT	2.473296 ± 0.10

FD-XAS measurements of S containing compounds in SWNTs against controls at the S K edge were acquired on beamline B28 at the ESRF. All measurements were obtained and room temperature and samples were prepared by mounting solid material on silicon (100) supports.

2. Raman Spectroscopy

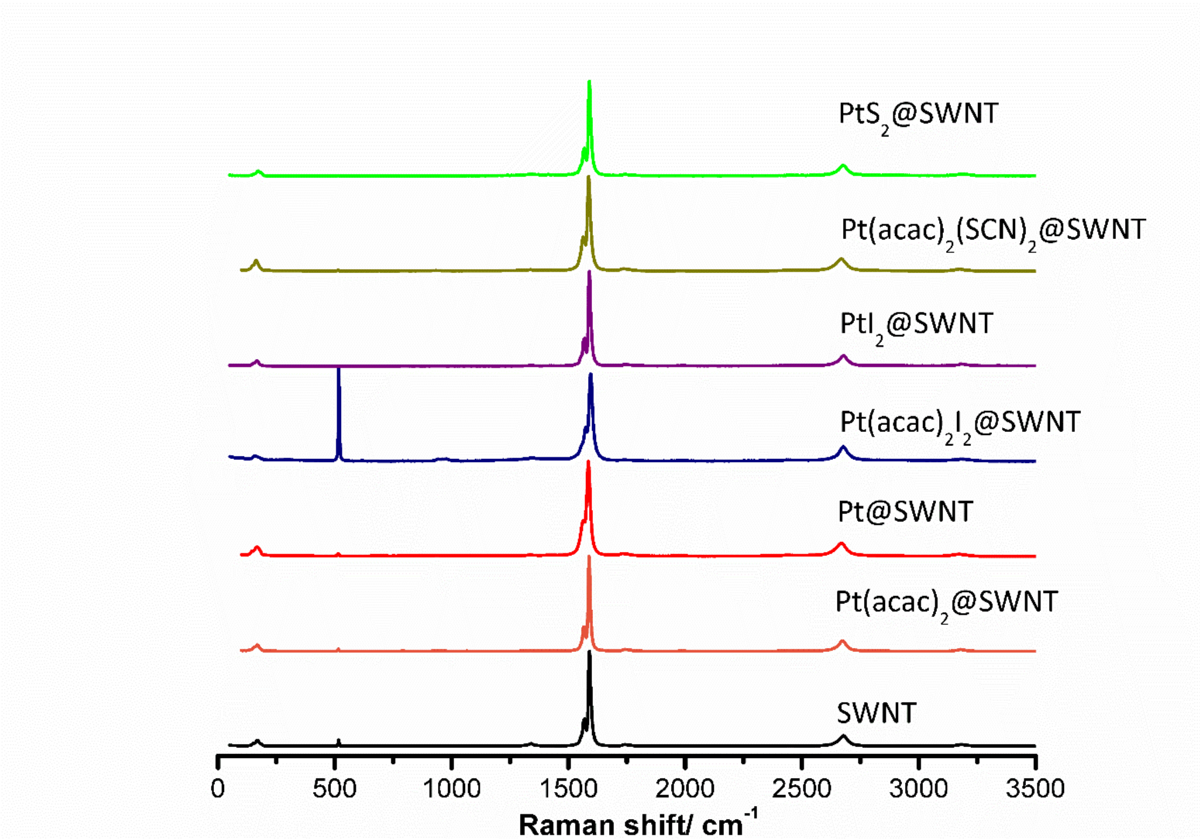

Figure S-6: Raman Spectra of all synthesised materials to show differences from that of an empty SWNT. All spectra were recorded at room temperature using a HoribaJY LabRAM HR spectro-meter, laser wavelength 532 nm. Samples were recorded by dispersing in propan-2-ol and drop-casting onto silicon (100) supports. The additional peal at 520.7 cm^{-1} in the spectrum of $Pt(acac)_2I_2$@SWNT is associated with the known optical phonon mode of the Si(100) support.

3. AC-HRTEM Data

a. Image simulation

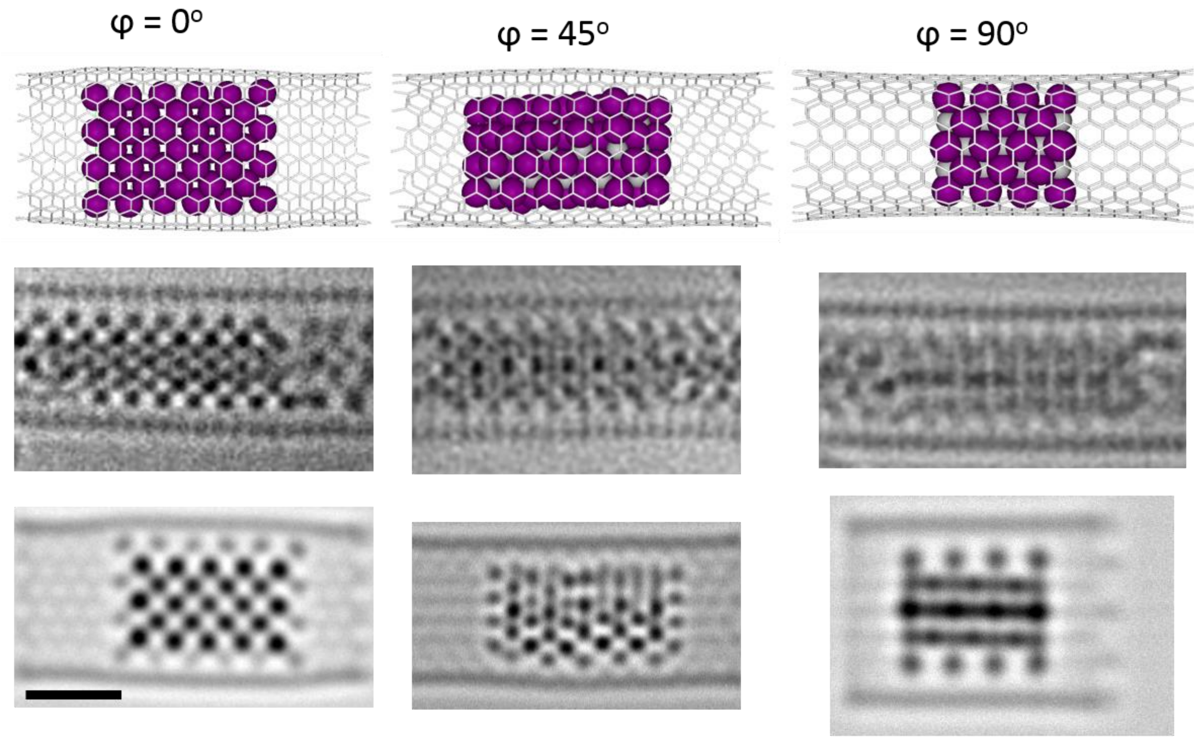

Figure S-7: Series showing a model of PtI_2@SWNT (top row) with the corresponding HR-TEM image (80 kV, middle row) and image simulation (QSTEM, 20 slices per image, bottom row). The model has been tilted by 45° (middle column) and 90° (right column). The corresponding HR-TEM images and subsequent simulations are shown underneath each model.

b. Additional AC-HRTEM images of PtI_2@SWNT

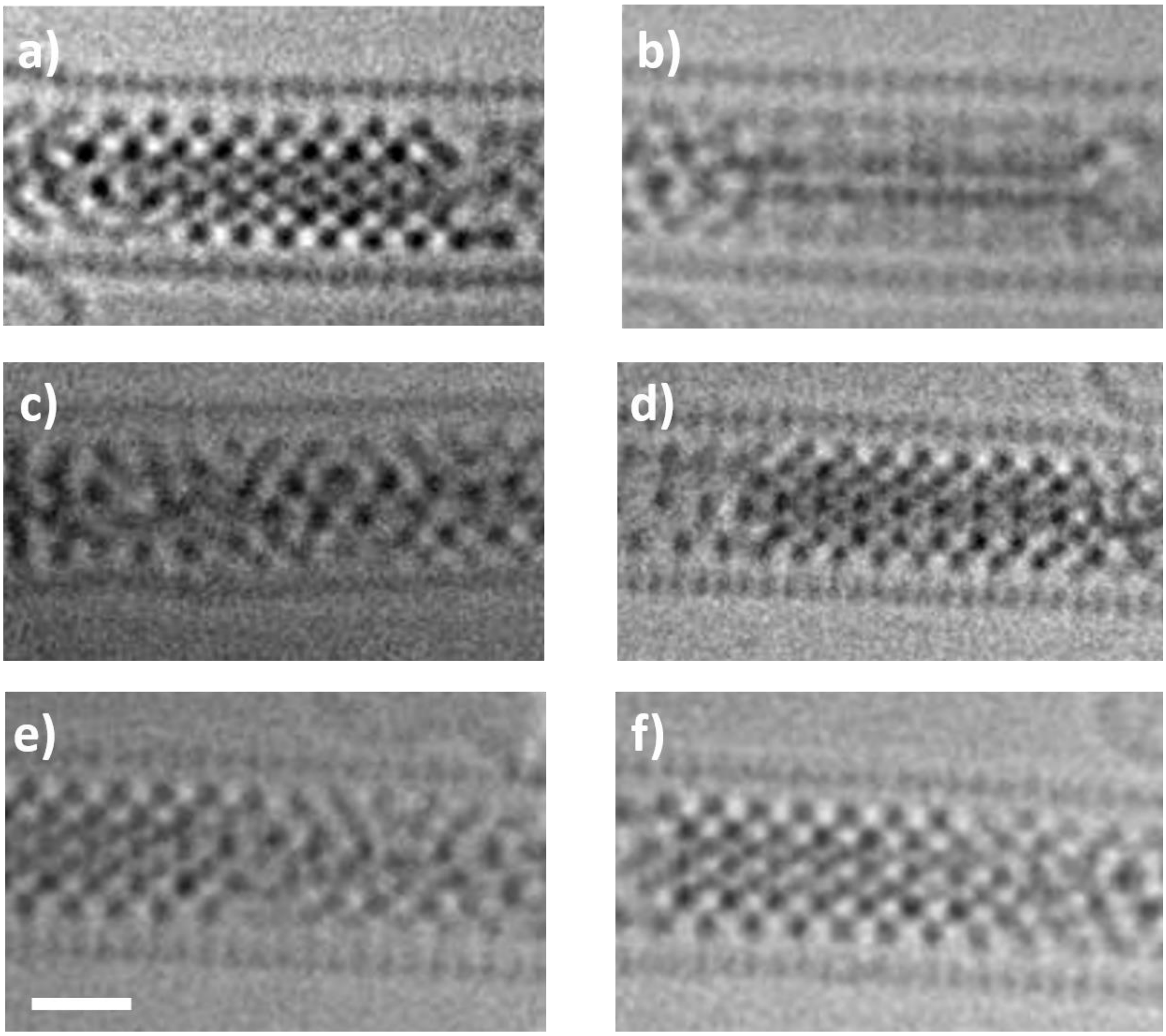

Figure S-8: (a-f) AC-HRTEM images (80 kV) showing different projections of PtI_2@SWNT. The scale bar is 0.5 nm.

c. Additional AC-HRTEM images of PtS_2@SWNT

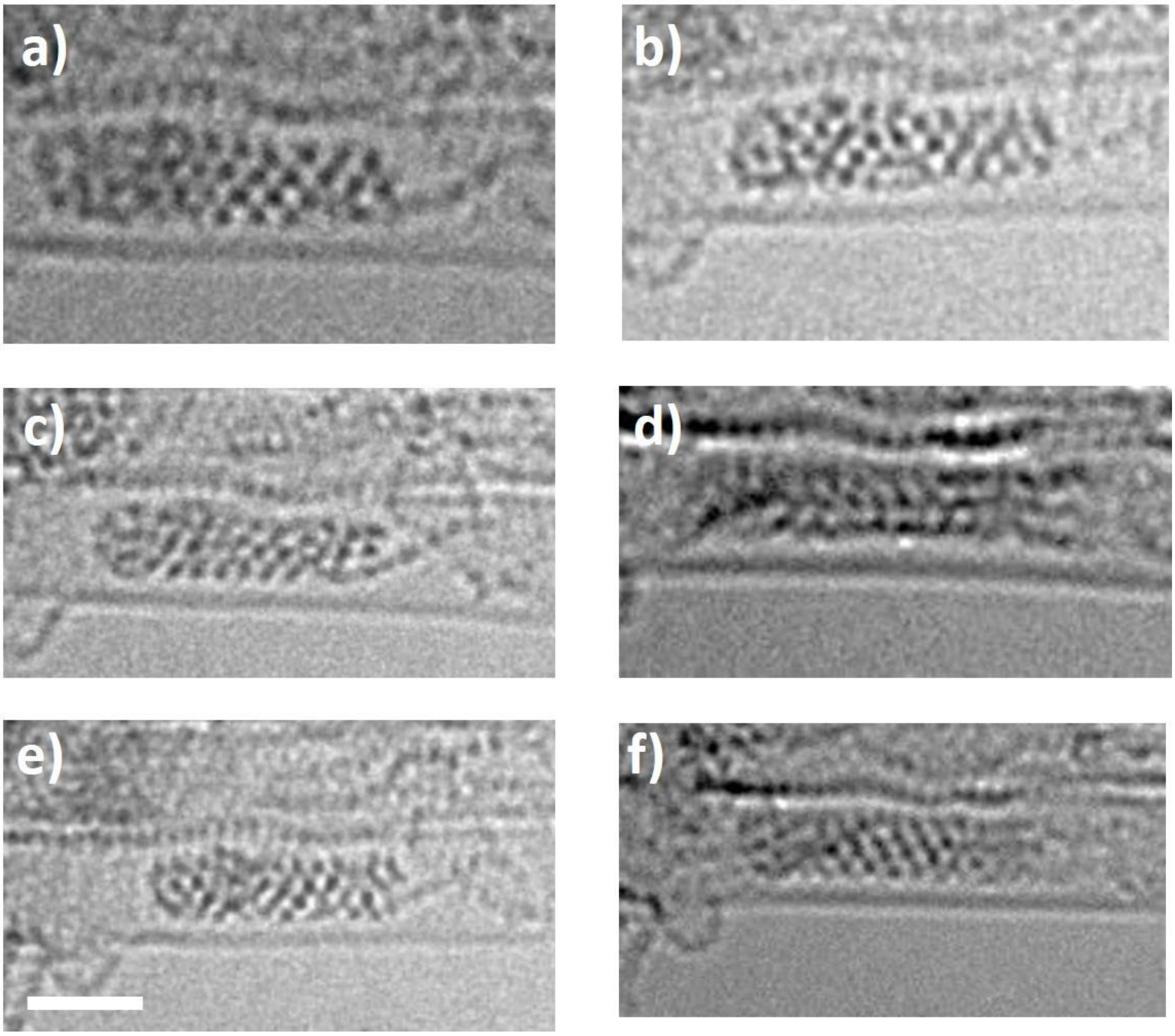

Figure S-9: (a-f) AC-HRTEM images (80 kV) showing different projections of PtS_2@SWNT. The scale bar is 1 nm.

d. AC-HRTEM images of Pt@SWNT

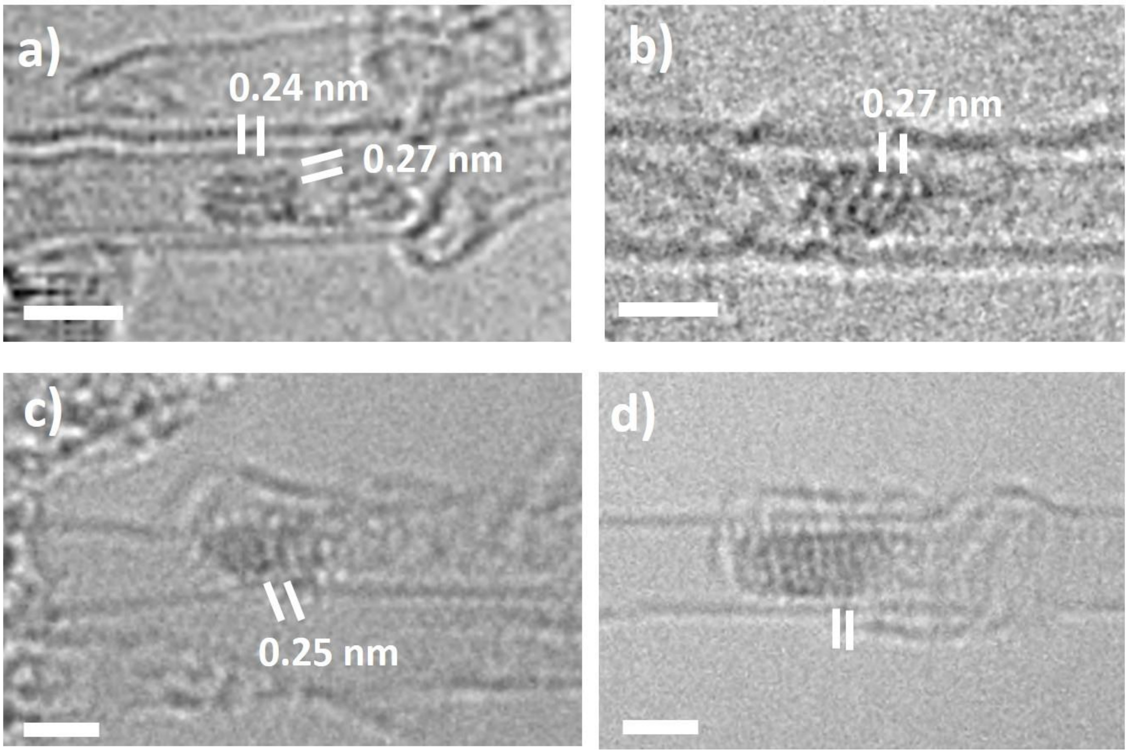

Figure S-10: (a-d) Representative AC-HRTEM images (80 kV) showing different examples of Pt@SWNT. The scale bars are all 1 nm. The interatomic distances between the Pt atoms are significantly shorter than those between Pt atoms in PtI_2@SWNT and PtS_2@SWNT (Figures 5c, 7a)

4. Development of PtI_2 structure

Bulk PtI_2 has a monoclinic unit cell with space group P2 (1)/c (figure S-10 a-c). A (11,11) SWNT, with a diameter of ca. 1.5 nm is shown for scale (figure S-11 d). The cubic structure from figure 5 b was derived from the asymmetric unit of PtI_2 (Figure S-10 e) which has been extended (figure S-10 f).

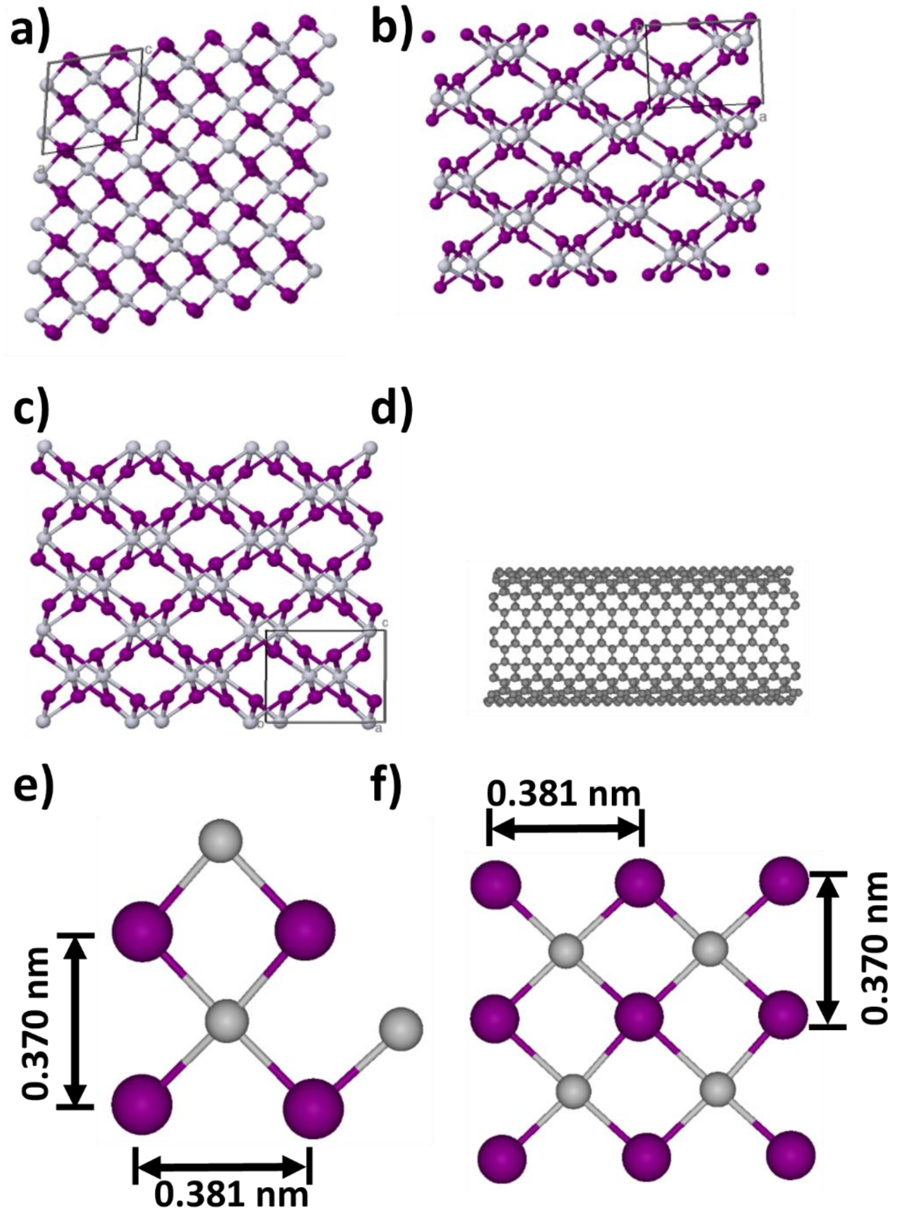

Figure S-11: a-c) Extended crystal structure of bulk PtI_2 in different orientations. PtI_2 as a monoclinic unit cell with space group P2 (1)/c; d) A (11,11) SWNT has a diameter of ca. 1.5 nm and is shown for scale; The cubic structure from figure 5 b was derived from the asymmetric unit of PtI_2 (e) which has been extended to form the basis of the cubic crystal plane (f).

The unit cell for bulk PtI_2 is 385.76 $Å^3$, with a measured density of 7.73 gcm^{-3}, which compares to a calculated density of ca. 11.60 gcm^{-3} for PtI_2@SWNT. This has been calculated as follows:

For a platinum diiodide crystal of formula $Pt_{28}I_{56}$ (figure S-12 a):

Mass= (195.1 $gmol^{-1}$ x 28) + (126.9 $gmol^{-1}$ x 56) = 11569.2 $gmol^{-1}$ = 2.087 x 10^{-20-} g.

The volume of the $Pt_{85}I_{56}$ unit has been approximated as follows:

The surface area of the crystal face looking down the nanotube (figure S-11 b):

(3.9 Å + 5.2Å) x 11.4 Å = 103.7 Å^{2}.

This is multiplied by the length of the crystal parallel to the nanotube (15.5 Å, figure S-11 a) giving a crystal volume of 1607.35 Å^{3}.

1.864 x 10^{-20} g /1607.35 Å^{3} = 11.60 gcm^{-3}.

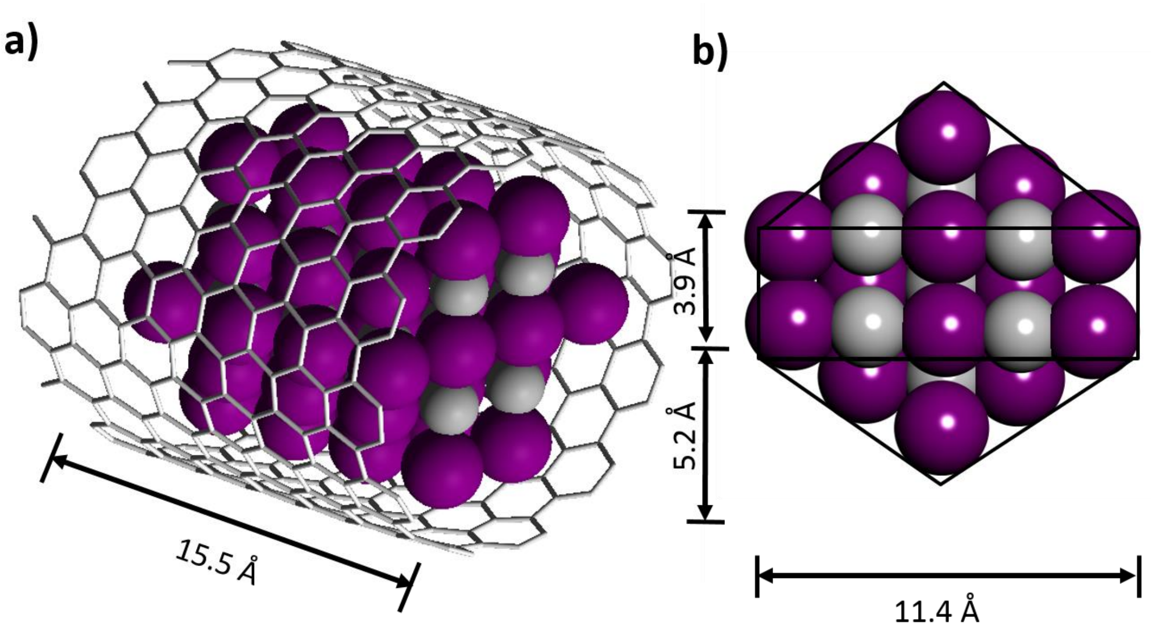

Figure S-12: A model of PtI_2@SWNT showing how density was calculated. A crystal of $Pt_{28}I_{56}$ of length 15.5 Å is inside a SWNT (a); b) the surface area of the crystal face was approximated using simple geometrical units and multiplied by the length of the crystal (15.5 Å). This gave a crystal volume of 1607.35 Å, which equates to a density of 11.60 gcm^{-3}.

Coordination number of each element:

Considering the smallest unit of our PtI_2@SWNT, Pt_7I_{14} (figure S-13).

Each Pt atom is coordinated to six I atoms, whereas the I atoms are coordinated to different amounts of Pt atoms depending on their position in the lattice, see the table below for full details

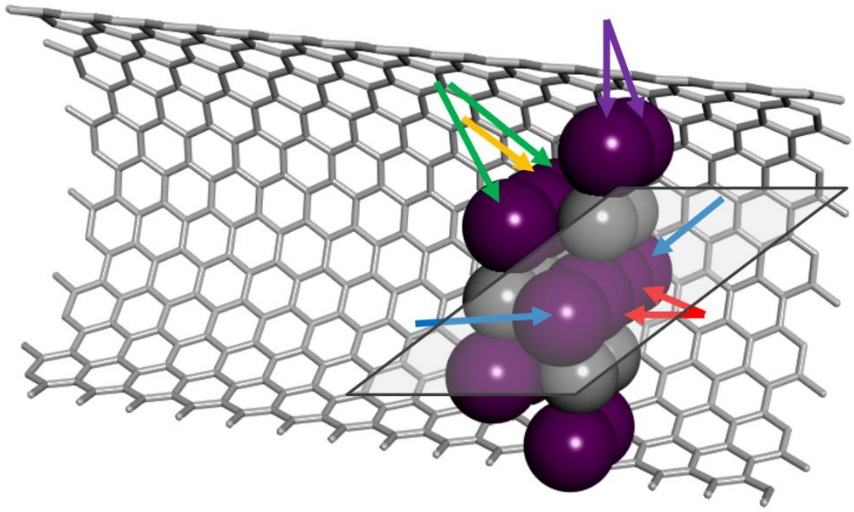

Figure S-13: Model of Pt_7I_{14}@SWNT showing the coordination number of each I atom. The purple arrow is showing the I atoms coordinated to one Pt atom (coordination number of one), the blue arrows shows the I atoms with a coordination number of two, the green arrow corresponds to I atoms with a coordination number of three, the yellow arrow to I atoms with a coordination number of five, and the red arrows to a coordination number of six. A mirror plane shows the symmetry and avoids the need to label the I atoms below with green, yellow or purple arrows.

Table S-4: coordination number of each type of I atom present and their frequency in the Pt_7I_{14} cell.

	Coordination number	Quantity of I atoms
(purple arrow)	1	4
(blue arrow)	2	2
(green arrow)	3	4
(yellow arrow)	5	2
(red arrow)	6	2

Average coordination number of each I atom: (4/14)x1 + (2/14)x2 + (4/14)x3 + (2/14)x5 + (2/14)x6 = 3

5. Quantitative EDX Analysis

The atomic ratios of elements in samples made using both a stepwise and one-pot approach have been quantified using EDX analysis. This involved taking representative spectra over a variety of areas of each sample and quantitatively evaluating the Pt:X (X = I, S) ratios.

Table S-5: Relative ratios of atoms in each sample as quantified using EDX analysis.

Element	Weight ratio	Atomic Ratio
Pt@SWNT + I_2 → PtI_x@SWNT		
Pt	1	**1**
I	3.67	**5.75**
PtI_x@SWNT + H_2S → PtS_x@SWNT		
Pt	1	**1**
S	4.06	**24.89**
I	0.80	**1.25**
$Pt(acac)_2I_2$@SWNT → PtI_2@SWNT		
Pt	1	**1**
I	1.35	**2.11**
$Pt(acac)_2(SCN)_2$@SWNT → PtS_2@SWNT		
Pt	1	**1**
S	0.32	**1.93**

For the stepwise synthesis of PtI_x@SWNT, there is a large excess of iodine, as shown by both the TEM images and EDX analysis, whereas the amount of iodine is greatly reduced during the one-pot synthesis. Similarly, treating PtI_x@SWNT with H_2S gas leads to a large excess of sulfur, compared to when the precursor $Pt(acac)_2(SCN)_2$ is decomposed.